空気調和・衛生工学会論文集
No. 146, 2009年5月

Numerical Simulation of Natural Ventilation of a Factory Roof Cavity

Lusi SUSANTI [*1], **Hiroshi HOMMA** [*2], **Hiroshi MATSUMOTO** [*3],
Yasumasa SUZUKI [*4], **and Masayuki SHIMIZU** [*5],

Synopsis: This study targets the reduction of solar heat gain by natural ventilation of a cavity in a factory roof. In the laboratory experiment [1], the average air velocity reached to 0.25m/s. A simulation program was developed to calculate the heat and air flow attained in the experiment. An airflow passage was divided into sections to trace the pattern of the air temperature rise. When the cavity was divided into 20 sections, it was enough to trace the temperature rise pattern, and hence to calculate buoyant force for natural ventilation. Then the simulated air velocities, temperatures rise and heat transportations were compared with the corresponding average values of the experimental results. The molecular viscosity and thermal conductivity of the air were modified to adjust the simulation results to the experimental results in the wide range of the experimental conditions. When they were multiplied with a magnitude of 30 equally, the root mean square of the ratio of deviations of the heat transportation became least. This simulation could predict the heat transportation as a result of natural ventilation with a root mean square of the deviation of 0.26 with a short calculation time.

Key words : Roof cavity, Natural ventilation, Air temperature, Air velocity, Viscosity, Thermal Conductivity, Adaptation

Introduction

To improve thermal environment in a factory and to reduce its cooling power consumption, it is more viable to prevent heat transfer through building claddings than to cool the penetrated heat by means of cooling installations. This holds true concerning with the initial investment and also the life cycle expense. The final purpose of this study was to know the heat evacuation performance of natural ventilation of a cavity roof. In the laboratory experiment, the average air velocity reached to 0.25m/s, where the experimental cavity configuration was a length of 4.88m, an inclination angle of 30 degrees, and an opening ratio of 45% at both the inlet and outlet [1]. This corresponded to an air turn over of 184 times a hour. The hot air was able to be dissipated and displaced with cool outdoor air. This suggested that the natural ventilation may be applied effectively to improve the thermal environment or to reduce the cooling load in a factory. Before to practice this technology in fields, the performance of natural ventilation should be examined under climatic conditions. For this purpose, numerical simulation of thermal load of a factory seemed an appropriate measure. To be included in this simulation, the heat transportation process of natural ventilation was discussed using the experimental results.

Most of researches on naturally ventilated roof were directed to residential houses and to the best of the authors' knowledge no data was published for natural ventilation of a factory roof. In Chapter 25 of 2005 ASHRAE Handbook of Fundamentals, the thermal resistances of airspaces of various configurations are tabulated. However, the base experiment for these data was conducted with no intention of ventilation [2].

A roof of an industrial building is long and its height is considerable. It raises considerable buoyant force on the air in the cavity when solar irradiation is transferred to the cavity. This buoyant force can be utilized favorably to dissipate the transferred heat outdoors by natural

*1 Department of Industrial Engineering, Andalas University
*2 Toyohashi University of Technology, Member
*3 Toyohashi University of Technology, Member
*4 Kakegawa Technical High School
*5 Sala-House Co., Ltd.

ventilation. In the present study, the characteristics of natural ventilation through a roof cavity were examined numerically comparing with the laboratory experimental results, where cavity surface temperature and velocity were measured with a heated model of various configurations by the authors [1]. A simple numerical simulation program was developed to express the natural ventilation performance, which could be adapted in a cooling/heating load calculation of a factory. This program was aimed at to be included in the thermal load calculation, which had to be repeated with a short time interval during a period of weather change.

1. Background

Many factories were built during the rapid industrial developmental period of several decades ago in South-Eastern Asia. They had a single cladding of corrugated asbestos cement boards. Their typical plan had a low inclination and widely spreading roof. In such a factory, the heat transfer of the roof had strong influence on the thermal environment and thermal load beneath it. In particular, the solar irradiation on the roof out-weighed the cooling load substantially, making the work space below unbearably hot, and causing reduction in work efficiency and quality.

These buildings have become aged and require expensive maintenance and repair work. Instead of repairing the roofs, roofers are developing measures to cover them totally with folded thin metal plates. When an old single roof is covered, a cavity is formed between the old roof and the new cover. If this cavity was ventilated, it would stop the penetration of solar radiation effectively and thus reduced the heat transfer into the work space.

Recently, new factories are being built in hot areas with high worker populations. As a result of the recent warming of the global atmosphere, industrial buildings, which require cooling in a summer, are sprawling in areas of higher latitude. The natural ventilation of a roof cavity can be employed in such new industrial buildings too.

The merits of this technique go beyond cooling load reduction. It is difficult to abandon asbestos including materials from the standpoint of environmental pollution. When an asbestos cement board is weathered on a roof, the cement component on the surface decays, which results in the disintegration of dangerous asbestos fibers, and they are dispersed into the atmosphere. When an asbestos cement board is covered, such weathering and dispersion are stopped.

2. Numerical model

To understand heat transportation by natural ventilation, its velocity and exit air temperature must be known. Both of heat and force exchange dictate the temperature and velocity of the cavity air ultimately. The temperature rise pattern has a significant effect in the heat evacuation performance of the natural ventilation. These terms may be calculated with simple linear equations of heat transfer and force balance, if the cavity is short. But it is hard to know the temperature rise pattern in a long cavity. For flow along a constant surface temperature or a constant heat flux inclined single plate, equations are available to calculate the pattern of the air temperature rise around it [3]. But in a long roof cavity, the temperature of the cavity internal surfaces varies, even though the heat fluxes on the external surface is constant, because of their thermal resistances. One measure to solve this problem is CFD. However, it requires a high speed computer and a long computing time.

To express the temperature rise pattern, the cavity was divided into a series of many sections along the direction of the airflow [4]. The exit air temperature in each section was elucidated by adopting the linear equations of heat transfer, where a temporary velocity was applied for the airflow. Repeating this procedure in each section from the inlet to the outlet successively, the temperature distribution and temperature of the air left the cavity were obtained.

The cavity was supposed to be a square duct in the velocity calculation model. In a long roof cavity, the natural convection on the upper and lower surfaces developed its thickness in a relatively short distance from the inlet. When the cavity was filled with the natural convection layers of the both surfaces, the flow was supposed to be treated as the same to duct flow. The air flow in the cavity was supposed to be one dimensional.

The heat balance in a section was supposed to be maintained by convection heat exchange between the upper and lower surfaces and the air, and by the heat transportation of the airflow as shown in **Fig. 1(a).** When the average temperature of the air in the cavity was warmer than the outside air, the buoyancy force pushed it to rise. Frictional loss on the cavity surfaces and the

geometry losses at the inlet and the outlet opposed the buoyancy force. The air movement in this space stabilized at the velocity when these forces balanced, as shown in **Fig. 1(b)**. To solve the balancing condition of the heat and air flow, the solution of the equations of heat and force balances were repeated correcting them alternatively.

2.1 Balance of energy

The temperature distribution of the cavity air was calculated as follows. The i th control section in the cavity was supposed to have a length of ΔL along the direction of the airflow and its width and depth were W and D, respectively. Initially, the air velocity was supposed to be u. The heat q_{in} brought into the section by the airflow was the product of specific heat of the air c, density of the air ρ, air velocity u, cavity sectional area $W \times D$, and the temperature of the entering air t_{i-1}. It is given as:

$$q_{in} = c\rho uWDt_{i-1} \qquad \cdots\cdots (1)$$

The heat q_{out} brought out from the section was calculated as follows

$$q_{out} = c\rho uWDt_i \qquad \cdots\cdots (2)$$

where t_i was the temperature of the air leaving the section. The subscript i stood for the number of the section, and $i = 0$ referred to the outside of the cavity from where the air entered. The heat transferred from the upper surface of the section was defined as:

$$q_u = h_u \Delta LW\left(t_{u(i)} - \frac{t_{(i-1)} + t_{(i)}}{2}\right) \qquad \cdots\cdots (3)$$

By the same consideration, the heat transferred from the lower surface was

$$q_l = h_l \Delta LW\left(t_{l(i)} - \frac{t_{(i-1)} + t_{(i)}}{2}\right) \qquad \cdots\cdots (4)$$

where h_u and h_l represented the convection heat transfer coefficient on the upper and lower surfaces, respectively. $t_{u(i)}$ and $t_{l(i)}$ represented the temperatures of the upper and the lower surfaces, respectively, of section i.

The natural convection heat transfer coefficients were calculated from the following equations of Nusselt number, respectively for horizontal heated plates facing downward and upward, supposing laminar flow [5] :

$$Nu_u = 0.27Ra^{1/4} \qquad \cdots\cdots (5)$$

$$Nu_l = 0.96Ra^{1/4} \qquad \cdots\cdots (6)$$

where the Rayleigh number Ra was evaluated from the following equation using the temperature difference between the respective surfaces and the average air temperature Δt in the section

$$Ra = g\beta\Delta tD^3 / \nu\alpha_t \qquad \cdots\cdots (7)$$

When the upper surface temperature was higher than the average air temperature in the section, the downward heat transfer coefficient was applied , and vice versa. The same way was applied for the lower surface.

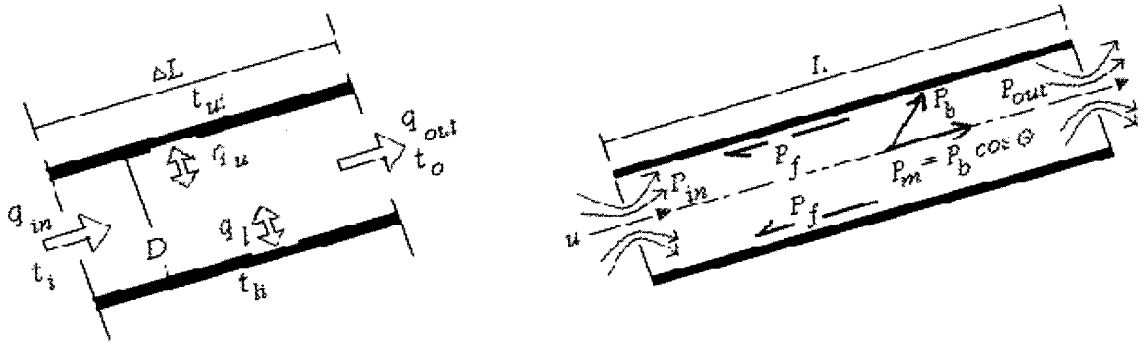

(**a**) Heat exchanges in a control space (**b**) Balance of forces

Fig. 1 Heat and force balances models in cavity

Consequently, the heat balance in the section was described by the following equation

$$q_{in} + q_u + q_l - q_{out} = 0 \qquad \cdots\cdots (8)$$

The temperature of the air left the section t_i was calculated from the above equation adapting the surface temperatures measured in the experiment.

2.2 Balance of forces

The buoyant pressure P_b which worked on the cavity air was the difference between the gravitational pressures caused on the outside air column of the same height as the cavity, and the gravitational pressure caused on the air in the cavity as

$$P_b = g\rho_0\left(\frac{273.15}{t_o+273.15}L\sin\theta - \sum_{i=1}^{n}\frac{273.15}{t_i+273.15}\Delta L\sin\theta\right) \qquad \cdots\cdots (9)$$

where the cavity was divided into n sections. The inclination direction element of the buoyant pressure, which was the motivational pressure P_m to flow the air through the cavity, was

$$P_m = P_b\sin\theta \qquad \cdots\cdots (10)$$

The dynamic pressure P_d of the airflow of a velocity of u was

$$P_d = \frac{1}{2}\rho_0 u^2 \qquad \cdots\cdots (11)$$

The geometric losses of the inlet and outlet were calculated, respectively as

$$P_{in} = k_{in}P_d \qquad \cdots\cdots (12)$$

$$P_{out} = k_{out}P_d \qquad \cdots\cdots (13)$$

where P_{in} was the pressure consumed at the inlet restriction, and P_{out} was it at the outlet restriction.

The geometric loss coefficients at the inlet k_{in} and outlet k_{out}, respectively were expressed by the following equations referred to the opening ratios of both the inlet and outlet, which were deduced from the loss coefficients at the inlet and outlet of the orifice of the ASHRAE Duct Fitting Data Base [6]

$$k_{in} = 1.0124\left(\frac{d_{in}}{D}\right)^{-3.137} \qquad \cdots\cdots (14)$$

$$k_{out} = 1.0049\left(\frac{d_{out}}{D}\right)^{-2.967} \qquad \cdots\cdots (15)$$

where d_{in} and d_{out} were the slit sizes of the inlet and outlet, respectively.

For fully developed laminar-viscous flow, the friction force due to contact with the cavity surfaces was a function of Reynolds Number $\mathrm{Re} = D_h u/\nu$, where ν was the molecular kinematic viscosity of the air and D_h was the hydraulic diameter of the cavity, which was evaluated by $\frac{4(D\times W)}{2(D+W)}$. So, the friction coefficient f was proportional to the viscosity ν as

$$f = \frac{64}{\mathrm{Re}} = \frac{64}{D_h u}\nu \qquad \cdots\cdots (16)$$

The frictional pressure loss was then

$$P_f = f\left(\frac{L}{D_h}\right)P_d = \frac{64\nu}{D_h u}\left(\frac{L}{D_h}\right)P_d \qquad \cdots\cdots (17)$$

where L was the total length of the cavity.

Consequently, the airflow of the cavity stabilized when motivational force P_m balanced with the three resisting forces as

$$P_m = P_{in} + P_{out} + P_f \qquad \cdots\cdots (18)$$

2.3 Simultaneous balance of temperature and velocity

In order to solve the balanced condition of heat and air flow in the air cavity, the equations of heat balance and force balance had to be solved simultaneously. The heat balance equations included the air velocity, and the force balance equation included the buoyancy, which was induced from the cavity air temperature distribution. As the heat balance equation was divided into many sections

and the equation of force balance was a binomial equation of the air velocity, it was difficult to solve these equations directly.

To attain the balanced condition of the two terms, the air temperature distribution was calculated with a supposed velocity firstly. Secondly, the buoyant force was calculated from the air temperature distribution, and the balance of forces was examined. These procedures started with a sufficiently low velocity. If the buoyant pressure was larger than the total of the three resisting pressures, the velocity was incremented by one step. In the presented program, a sufficiently low velocity was assumed initially, and the velocity increment step was set at 0.001 m/s. This procedure was repeated until the pressure balance equation (18) crossed zero.

2.4 Effect of number of sections

As the number of sections became larger, the temperature rise pattern was traced more accurately. Although, the larger the section number was, the more the computation time was required. A suitable section number was sought using the above program. In this calculation, the configuration of the cavity was a length of 20m, a depth of 78mm, a width of 400mm, and an inclination angle of 30 degrees. The supposed temperatures were an ambient temperature of 25°C, an upper surface temperature of 40°C and a lower surface temperature of 35°C. **Fig. 2** shows the temperature rise patterns of various section numbers. When the cavity was divided into more than 5 sections, the temperature rise pattern was smooth. **Fig. 3** shows the outlet temperature and the average temperature rises in the cavity, which related to the buoyant force. The number on top of each outlet temperature was the proportion of it to the average temperature of corresponding section number. The velocities for various section numbers are shown in **Fig. 4**. The velocity increased with the increase of the section number. The number on top of each velocity was the proportion of the velocity to it of section number of 100. **Fig. 5** shows the heat transported out of the cavity by the natural ventilation. The heat transportation was the highest with the section number of one. The thermal balance and force balance were held by the combination of the highest exit temperature and the lowest velocity even in this case. The number at the top of each column was the proportion of the heat transportation to it of section number of 100.

These figures show that when the section number was larger than 20, the deviations in the temperature rise, velocity and heat transportation were less than 0.1% from those of section number of 100. So a section number of 20 was chosen for the following numerical examination.

3. Comparison of Experimental and Simulation Results

3.1 Simulation procedure

Reynolds numbers of the all experimental cases were shown in **Table 1**, which was published in reference 1. These indicated that the flow was laminar in all the experiment. Therefore, firstly the flow simulation was executed with the laminar heat transfer coefficient evaluated by Equations (5) and (6), and the molecular viscosity of the air. However, the simulation indicated that the temperature rise was excessively lower than the average temperature rise of the experiment, and the velocity was excessively faster than the average velocity of the experiment, in each corresponding case.

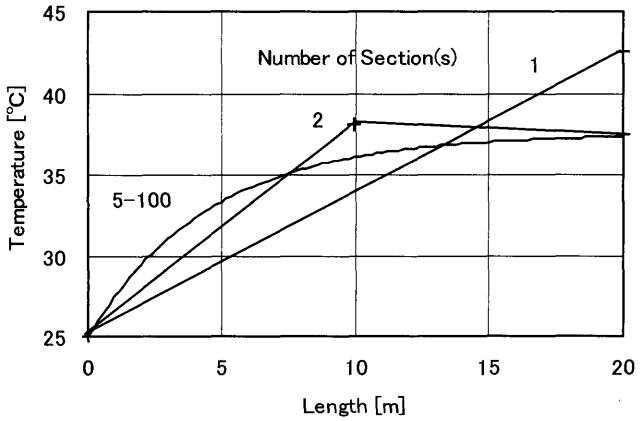

Fig. 2 Change of temperature rise with section number

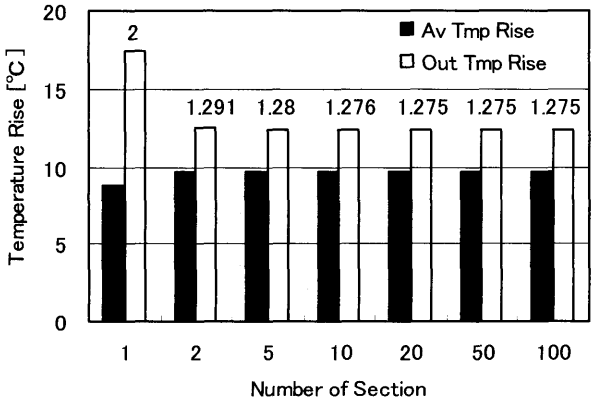

Fig. 3 Outlet and average temperature rises

One of the authors made a measurement of the velocity and temperature distributions of the natural ventilation in vertical wall cavities, and compared them with the results of numerical simulation[7]. In this comparison it was suggested that the viscosity and thermal conductivity of the air should be increased to reproduce the patterns of the simulated velocity and temperature distributions to their corresponding patterns of the experiment.

Fluid may have to travel a length equal to 60 times the diameter of a pipe before the stable pattern of flow corresponding to the particular Reynolds number is established. The pressure drop per unit length for a particular velocity is greater for turbulent flow than for laminar flow. The dissipation of energy in turbulent flow consequently occurs at a greater rate than in laminar flow, even at the same mean velocity [8].

When turbulence takes place, the main momentum and heat exchange mechanism is one involving lateral movement of macroscopic lumps of fluid in the flow [9]. In a fully turbulent region we speak of eddy viscosity and eddy thermal conductivity. In turbulent flow we must deal with these eddy properties instead of the ordinary molecular thermal conductivity and viscosity.

From these facts, turbulence was supposed to include in the present flow. The present experimental model had an equivalent diameter of 0.13 m and a length of 4.882 m. This suggested that the flow in the cavity was in an transient state between laminar and turbulent flow. Turbulence might be brought into the cavity by the entered flow, and might be arisen at the entrance. It might take the whole length of the experimental model before it attained a laminar state. Then the resistance of flow was greater, and the heat transfer coefficient was also greater than in laminar flow. For fully developed flow, models were presented to evaluate these two terms [10]. But no data was found for such a low Reynolds number and trancient state flow as in the present experiment. So these values were searched for in the following way. To adjust the calculated values with the experimental results in the wide range of the experimental conditions, the molecular viscosity and the heat transfer coefficients were corrected as follows.

For fully developed turbulent flow, Plandtl suggested the following equation for a model of turbulent viscosity μ_T in 1920's [11].

$$\mu_T = \rho l^2 \left| \frac{\delta u}{\delta y} \right| \qquad \cdots\cdots (19)$$

where l , a "mixing length," can be thought of as a traverse distance over which particles maintain their original momentum, somewhat on the order of a mean free path for the collision or mixing of globules of fluid. The product $l|\delta u / \delta y|$ can be interpreted as the characteristic velocity of turbulence, u is the component of velocity in the primary flow direction and y is the coordinate transverse to the primary flow direction.

A turbulent kinematic viscosity ν_T , which was the quotient of a dynamic viscosity divided by the specific mass, was estimated as the upper limit of the viscosity of the present experiment adapting the experimental conditions into equation (19). A half of the hydraulic diameter of the experimental model was applied to the mixing lengths y and l. The average velocity of 0.18m/s of the experiment with two openings of 35mm, a

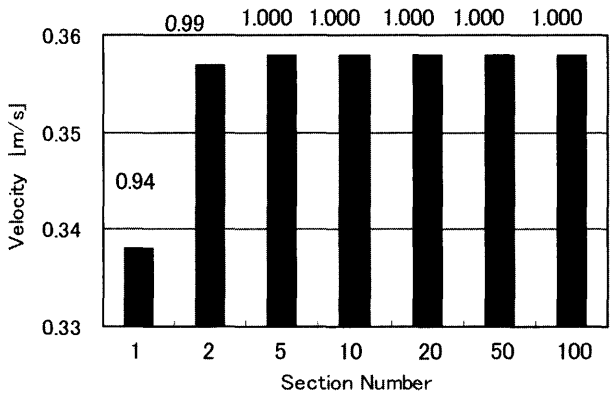

Fig. 4 Change of velocity with section number

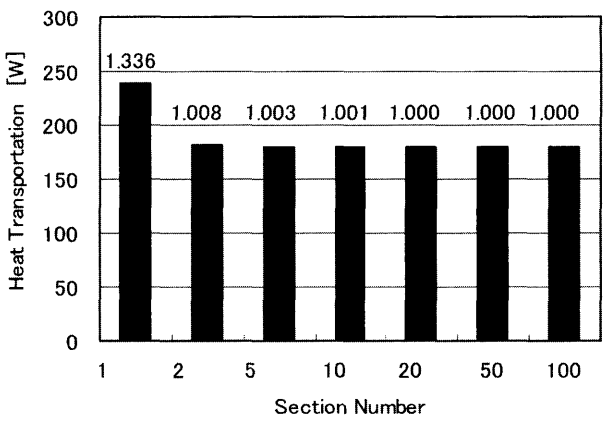

Fig. 5 Change of heat transportation with section number

heat production of 150W/m^2 and an inclination angle of 30 degrees, was applied to the velocity u. The velocity gradient was replaced by the quotient of the average velocity divided by the mixing length l .The estimation yielded the turbulent viscosity to be 0.014 Pa This was 900 times larger than the molecular viscosity. The magnitude of the viscosity had to be between unity and this value in the present experiment. As the flow in the present experiment was much lower than that fully developed turbulent flow, the viscosity in the experiment was supposed to be in the nearer side to unity.

About the turbulent thermal conductivity, the following discription was found. "In turbulent flow, the additional transportation of heat is caused by the turbulent motion. Experiment confirm that the ratio of the diffusivities for the turbulent transport of heat and momentum is an well-behaved function across the flow [12)]."

Table 1 Comparison of experimental and simulation results

experimental model				experimental				simulated			deviation
heat prod.	inlet open.	outlet open.	amb. Temp.	aver. vel.	aver. temp. rise	heat transp.	Re	vel	temp. rise	heat transp.	in heat transp.
[W/m^3]	[mm]	[mm]	[°C]	[m/s]	[°C]	[W]		[m/s]	[°C]	[W]	[W]
30 deg.											
150	78	78	12.2	0.246	22.6	103.2	1599	0.156	29.1	95.4	0.006
100	78	78	13.3	0.228	20.5	65.0	1428	0.131	27.5	55.8	0.020
75	78	78	12.5	0.211	19.2	57.7	1338	0.123	25.5	45.9	0.042
50	78	78	12.6	0.179	18.0	37.2	1159	0.100	23.3	25.9	0.092
150	78	35	12.1	0.198	27.9	123.2	1371	0.147	30.8	113.7	0.006
100	78	35	12.7	0.180	24.6	85.9	1240	0.126	28.2	71.2	0.029
75	78	35	13.9	0.142	23.8	56.1	1159	0.114	28.0	50.8	0.009
50	78	35	13.8	0.121	21.6	35.7	1053	0.101	26.0	35.4	0.000
150	78	20	14.2	0.136	34.5	108.2	971	0.113	35.5	105.0	0.001
100	78	20	14.5	0.107	31.4	71.1	889	0.100	32.8	74.3	0.002
75	78	20	14.4	0.099	28.4	42.5	832	0.093	30.6	55.7	0.096
50	78	20	14.3	0.094	24.3	28.1	759	0.082	27.7	34.6	0.054
150	78	10	15.9	0.111	43.5	119.2	490	0.058	42.1	69.8	0.172
100	78	10	16.7	0.090	37.0	70.4	441	0.051	37.8	44.3	0.137
75	78	10	17.3	0.087	34.3	46.0	416	0.048	36.4	33.9	0.069
50	78	10	19.1	0.072	32.1	29.7	383	0.044	36.2	23.2	0.048
150	35	35	13.6	0.129	30.7	91.8	1110	0.143	33.2	115.5	0.067
100	35	35	14.0	0.124	26.6	65.5	1012	0.121	30.0	69.9	0.005
75	35	35	14.3	0.108	25.1	48.8	955	0.111	28.9	53.6	0.010
50	35	35	14.8	0.104	23.3	30.9	897	0.100	27.9	37.1	0.040
150	20	20	14.9	0.063	37.5	96.3	636	0.101	38.0	102.7	0.004
100	20	20	15.5	0.090	33.6	64.6	596	0.091	35.4	72.0	0.013
75	20	20	16.1	0.075	31.2	44.7	563	0.084	33.8	54.2	0.045
50	20	20	16.1	0.060	27.2	26.3	530	0.075	30.9	33.9	0.084
150	10	10	19.3	0.063	50.4	76.9	294	0.056	49.1	71.5	0.005
100	10	10	19.0	0.053	42.3	50.7	277	0.051	43.1	47.9	0.003
75	10	10	19.6	0.054	38.7	40.5	261	0.047	41.2	35.8	0.013
50	10	10	19.7	0.044	34.2	18.3	237	0.043	38.0	24.3	0.107
20 deg.											
150	78	78	23.3	0.213	35.8	102.0	2309	0.096	46.1	64.8	0.133
100	78	78	20.8	0.190	30.5	74.8	2056	0.081	39.6	41.4	0.199
75	78	78	21.4	0.174	29.3	54.0	1974	0.074	38.3	29.5	0.206
50	78	78	20.0	0.168	26.1	35.3	1819	0.065	34.6	20.2	0.183
150	78	35	21.9	0.166	39.2	112.0	1477	0.091	45.8	74.9	0.110
100	78	35	20.8	0.153	33.5	79.1	1338	0.078	40.4	46.0	0.175
75	78	35	21.0	0.137	31.3	47.8	1281	0.072	38.9	34.4	0.079
50	78	35	20.6	0.105	27.9	33.8	1191	0.062	35.7	20.2	0.162
150	78	20	22.6	0.120	44.6	104.1	857	0.074	48.7	71.2	0.100
100	78	20	21.9	0.113	38.7	68.9	791	0.065	43.6	46.8	0.103
75	78	20	23.4	0.115	36.9	48.6	759	0.060	43.1	34.2	0.088
50	78	20	22.1	0.087	31.8	30.4	702	0.054	39.1	22.1	0.075
150	35	35	22.2	0.124	40.9	94.0	1134	0.090	47.4	79.0	0.025
100	35	35	22.0	0.109	35.7	63.0	1036	0.077	42.7	48.4	0.054
75	35	35	23.2	0.087	34.0	43.1	1012	0.071	42.0	34.8	0.037
50	35	35	24.0	0.076	31.8	29.0	971	0.065	40.8	22.9	0.044
										RMS	0.259

In laminar flow, the friction coefficient f was proportional to the molecular kinematic viscosity v as shown in equation (16), and the heat transfer coefficient was proportional to the molecular thermal conductivity. So the frictional coefficient and the heat transfer coefficient were multiplied with the same magnitude.

3.2 Simulation results

Table 2 Simulation results with pressure loss shares

experimental model				simulation result						
H. prod.	Inlet	Outlet	Tamb	Vel	Tav	H. Trns.	Pressure			
							Buoy.	L inlet	L outlet	L frlct
[W]	[mm]	[mm]	[°C]	m/s	[°C]	[W]	[Pa]	[Pa]	[Pa]	[Pa]
30 deg.										
150	78	78	12.2	0.156	29.1	95.4	0.759	0.001	0.014	0.745
100	78	78	13.3	0.131	27.5	55.8	0.632	0.001	0.010	0.624
75	78	78	12.5	0.123	25.5	45.9	0.593	0.001	0.009	0.587
50	78	78	12.6	0.100	23.3	25.9	0.480	0.000	0.006	0.477
150	78	35	12.1	0.147	30.8	113.7	0.838	0.001	0.136	0.703
100	78	35	12.7	0.126	28.2	71.2	0.699	0.001	0.099	0.601
75	78	35	13.9	0.114	28.0	50.8	0.623	0.000	0.081	0.541
50	78	35	13.8	0.101	26.0	35.4	0.538	0.000	0.064	0.480
150	78	20	14.2	0.113	35.5	105.0	0.946	0.000	0.419	0.536
100	78	20	14.5	0.100	32.8	74.3	0.801	0.000	0.327	0.474
75	78	20	14.4	0.093	30.6	55.7	0.717	0.000	0.283	0.441
50	78	20	14.3	0.082	27.7	34.6	0.606	0.000	0.220	0.389
150	78	10	15.9	0.058	42.1	69.8	1.100	0.000	0.857	0.274
100	78	10	16.7	0.051	37.8	44.3	0.882	0.000	0.661	0.240
75	78	10	17.3	0.048	36.4	33.9	0.789	0.000	0.584	0.225
50	78	10	19.1	0.044	36.2	23.2	0.687	0.000	0.488	0.205
150	35	35	13.6	0.143	33.2	115.5	0.876	0.073	0.128	0.680
100	35	35	14.0	0.121	30.0	69.9	0.715	0.052	0.091	0.575
75	35	35	14.3	0.111	28.9	53.6	0.641	0.044	0.077	0.526
50	35	35	14.8	0.100	27.9	37.1	0.568	0.036	0.062	0.473
150	20	20	14.9	0.101	38.0	102.7	0.984	0.177	0.334	0.478
100	20	20	15.5	0.091	35.4	72.0	0.843	0.144	0.270	0.430
75	20	20	16.1	0.084	33.8	54.2	0.746	0.122	0.230	0.396
50	20	20	16.1	0.075	30.9	33.9	0.633	0.097	0.183	0.354
150	10	10	19.3	0.056	49.1	71.5	1.191	0.154	0.790	0.261
100	10	10	19.0	0.051	43.1	47.9	0.996	0.128	0.656	0.238
75	10	10	19.6	0.047	41.2	35.8	0.868	0.109	0.556	0.219
50	10	10	19.7	0.043	38.0	24.3	0.731	0.091	0.465	0.200
20 deg.										
150	78	78	23.3	0.096	46.1	64.8	0.447	0.000	0.005	0.442
100	78	78	20.8	0.081	39.6	41.4	0.378	0.000	0.004	0.376
75	78	78	21.4	0.074	38.3	29.5	0.342	0.000	0.003	0.343
50	78	78	20.0	0.065	34.6	20.2	0.301	0.000	0.002	0.302
150	78	35	21.9	0.091	45.8	74.9	0.469	0.000	0.050	0.421
100	78	35	20.8	0.078	40.4	46.0	0.394	0.000	0.037	0.362
75	78	35	21.0	0.072	38.9	34.4	0.360	0.000	0.032	0.334
50	78	35	20.6	0.062	35.7	20.2	0.308	0.000	0.023	0.288
150	78	20	22.6	0.074	48.7	71.2	0.508	0.000	0.174	0.341
100	78	20	21.9	0.065	43.6	46.8	0.429	0.000	0.135	0.300
75	78	20	23.4	0.060	43.1	34.2	0.390	0.000	0.114	0.276
50	78	20	22.1	0.054	39.1	22.1	0.342	0.000	0.093	0.249
150	35	35	22.2	0.090	47.4	79.0	0.493	0.028	0.049	0.415
100	35	35	22.0	0.077	42.7	48.4	0.411	0.021	0.036	0.356
75	35	35	23.2	0.071	42.0	34.8	0.373	0.017	0.030	0.327
50	35	35	24.0	0.065	40.8	22.9	0.334	0.015	0.025	0.298

Various magnitudes were multiplied to the viscosity and heat transfer coefficient equally, and the velocity, temperature rise and the heat transportation of the airflow were calculated using the simulation program. The deviation ratios of the simulated heat transportations from those of the corresponding experimental results divided by the latter were calculated. The root mean squares of them were sought for the experimental cases, where the outlet opening was smaller than or equal to the inlet opening. The opposite cases were excluded from this calculation, because counter flow was supposed at the outlet [13]. The smallest RMS was found at a multiple magnitude of 30. This indicated that the simulation could predict the experimental heat transportation with the least deviations when the viscosity and the thermal conductivity was multiplied by 30. The velocities, temperature rises and heat transportations in the experiment and the simulation, and their deviations at the multiple magnitude of 30 are shown in **Table 1**.

The buoyancy, losses at the inlet and outlet and friction loss were calculated in the simulation, which were shown in columns 9, 10 and 11, respectively in **Table 2**. In the case of an heat production of 150W/m^2, inlet and outlet openings of 35mm, the shares of the pressure loss were 0.078, 0.135 and 0.699 Pa, respectively. This meaned a large portion of the buoyant pressure were consumed by the frictional resistance.

4. Conclusions

A numerical simulation model was developed to predict the ventilation effect of solar heat dissipation. When the cavity was divided into twenty sections, the temperature rise pattern was traced with a deviation of less than 0.1% compared with the calculation of one hundred sections.

The Reynold number suggested that the flow was laminar. However, the air flow was in an intermediate or transient state between laminar and turbulent flow judging from the temperature and airflow calculation with laminar heat transfer coefficient and molecular viscosity. The heat transfer coefficient and the viscosity had to be increased by a multiple magnitude of 30 to attain the least RMS of the deviations of the simulated heat transportation from the experimental results. By this mean, the simulation model was able to predict the heat transportation of the natural ventilation in the experiment with a RMS of 0.26.

The simulation indicated that the frictional pressureloss took the largest part in the considered three resistances.

Acknowledgement

This study was supported in part by the 21st Century COE Program "Ecological Engineering for Homeostatic Human Activities", from the Ministry of Education, Culture, Sports, Science and Technology, Japan.

References

1) L. Susanti, H. Homma, H. Matsumoto, Y. Suzuki and M. Shimizu, A Laboratory Experiment on Natural Ventilation of Roof Cavity, Trans.SHASE, No. 135, June 2008, pp.27-35

2) ASHRAE Handbook of Fundamentals. Atlanta: American Society of Heating, Refrigerating, and Air-Conditioning Engineers, Inc, 2005, pp. 25.4.

3) Holman, J. P. Heat Transfer. McGraw-Hill. Fifth Edition, 1981, pp. 274-281.

4) Homma, H. Solar Radiation Dissipation of a Double Sawtooth Roof by Natural convection, Meeting Papers 2001 D-2, Architectural Institute of Japan, pp.485-488 (in Japanese)

5) ASHRAEHandbook–Fundamentals. Atlanta: American Society of Heating, Refrigerating, and Air-Conditioning Engineers, Inc, 2005, p. 3.17

6) ASHRAE Duct Fitting Database–CD ROM. Atlanta: American Society of Heating, Refrigerating, and Air-Conditioning Engineers, Inc, 2002.

7) Homma, H et al., Natural Ventilation of Wall Air Cavity for Solar Heat Gain Reduction, Part 2 Calculation method of heat and air transfer in cavity, Trans. SHASE, No.30, 1986, pp.103-114 (in Japanese)

8) Massey, B.S., Mechanics of Fluids 2nd Edition, Van Nostrand Reihold Company, London, 1968, pp.132-133.

9) Holman, J. P. Heat Transfer. McGraw-Hill. Fifth Edition, 1981, p.196.

10) Anderson, D.A., Tannehill, J.C., and Pletcher, R.H. Computational Fluid Mechanics and Heat Transfer, Series in computational methods in mechanics and thermal sciences, Hemisphere Publishing corporation, New York, 1984, pp.221-235

11) Anderson, D.A., Tannehill, J.C., and Pletcher, R.H. Computational Fluid Mechanics and Heat Transfer, Series in computational methods in mechanics and thermal sciences, Hemisphere Publishing corporation,

New York, 1984, p. 222

12) Anderson, D.A., Tannehill, J.C., and Pletcher, R.H., Computational Fluid Mechanics and Heat Transfer, Series in computational methods in mechanics and thermal sciences, Hemisphere Publishing corporation, New York, 1984, p. 225

13) Susanti, Lusi et al., Effect of natural ventilation of a factory roof on cooling load reduction, Meeting papers of SHASE, Aug. 2005, F-16

Nomenclatures

c : Specific heat of air, [(J/kg・K)]
d : Opening restriction, [m]
D : Cavity thickness, [m]
D_h : Hydraulic diameter of cavity, [m]
f : Friction loss coefficient
g : Gravitational acceleration, [m/s^2]
h : Convection heat transfer coefficient, [W/(m^2・K)]
k : Losses coefficient
L : Cavity length, [m]
ΔL : Section length, [m]
Nu : Nusselt number
P : Pressure, [N/m^2]
q : Heat flux, [W/m^2]
Ra : Rayleigh number
t : Temperature, [°C]
Δt : Temperature difference, [°C]
u : Air velocity, [m/s]
W : Cavity width, [m]

Greek symbols

θ : Inclination angle of roof, [°]
β : Expansion coefficient, [1/K]
ρ : Density of air, [kg/m^3]
ν : Kinematic viscosity, [m^2/s]
α_t : Thermal diffusivity, [m^2/s]

Subscripts

0 : air at 0 °C
b : buoyant pressure element
d : dynamic force
f : frictional
i : section
l : lower surface
o : outdoor air
m : inclination direction element of buoyant pressure
u : upper surface
in : inlet of cavity
out : outlet of cavity

(Received December 8, 2008)

工場屋根内中空層の自然換気の数値シミュレーション

ルーシー スーサンティ[*1] 本間 宏[*2] 松本 博[3*] 鈴木 康政[*4] 清水 雅之[*5]

キーワード：屋根内中空層・自然換気・空気温度・気流速度・粘性係数・熱伝導率・適合

この研究は、工場の屋根内で中空層の自然換気を利用して日射熱取得を低減することを目的としている。実験室実験[1)]において平均流速は0.25m/sに達した。この実験で得られた上下の表面温度から気流とその輸送熱流を計算するためのシミュレーションプログラムを作成した。空気温度の上昇を追跡するために中空層を流れに沿って複数の節に分割する方法を取った。中空層を20節に分割した場合、空気温度上昇過程とこれによる自然換気の浮力の計算が充分に追跡された。実験で得られた中空層内の気流はレイノルズ数から判断すれば層流の範囲にあったが、空気の分子粘性係数と熱伝導率を用いてこのプログラムで計算した値は実験結果よりも流速は早く、温度上昇は少ないことが分かった。広い範囲の実験条件で、計算結果を実験結果に適合させるために、空気の分子粘性係数と熱伝達率の修正を行った。両者を30倍した時に熱輸送の偏差の二乗平均値が最小になることが分かった。この近似は短い計算時間で自然換気による熱輸送を誤差の二乗平均値 0.26 で予測できる。

（平成20. 12. 8 原稿受付）

*1 アンダラス大学産業工学科
*2 豊橋技術科学大学 正会員
*3 同大学建設工学系 正会員
*4 掛川工業高等学校
*5 ㈱サーラ住宅